Optical Engineering

OpticalEngineering.SPIEDigitalLibrary.org

Microoptoelectromechanical systems-based external cavity quantum cascade lasers for real-time spectroscopy

Lorenz Butschek
Stefan Hugger
Jan Jarvis
Marko Haertelt
André Merten
Markus Schwarzenberg
Jan Grahmann
David Stothard
Matthew Warden
Christopher Carson
John Macarthur
Frank Fuchs
Ralf Ostendorf
Joachim Wagner

Lorenz Butschek, Stefan Hugger, Jan Jarvis, Marko Haertelt, André Merten, Markus Schwarzenberg, Jan Grahmann, David Stothard, Matthew Warden, Christopher Carson, John Macarthur, Frank Fuchs, Ralf Ostendorf, Joachim Wagner, "Microoptoelectromechanical systems-based external cavity quantum cascade lasers for real-time spectroscopy," *Opt. Eng.* **57**(1), 011010 (2017), doi: 10.1117/1.OE.57.1.011010.

Microoptoelectromechanical systems-based external cavity quantum cascade lasers for real-time spectroscopy

Lorenz Butschek,[a,*] Stefan Hugger,[a] Jan Jarvis,[a] Marko Haertelt,[a] André Merten,[b] Markus Schwarzenberg,[b] Jan Grahmann,[b] David Stothard,[c] Matthew Warden,[c] Christopher Carson,[c] John Macarthur,[c] Frank Fuchs,[a] Ralf Ostendorf,[a] and Joachim Wagner[a]

[a]Fraunhofer Institute for Applied Solid State Physics IAF, Department for Optoelectronics, Freiburg, Germany
[b]Fraunhofer Institute for Photonic Microsystems IPMS, Department for Active Microoptical Devices and Systems, Dresden, Germany
[c]Fraunhofer Centre for Applied Photonics, Glasgow, United Kingdom

Abstract. We report on mid-IR spectroscopic measurements performed with rapidly tunable external cavity quantum cascade lasers (EC-QCLs). Fast wavelength tuning in the external cavity is realized by a microoptoelectromechanical systems (MOEMS) grating oscillating at a resonance frequency of about 1 kHz with a deflection amplitude of up to 10 deg. The entire spectral range of the broadband QCL can therefore be covered in just 500 μs, paving the way for real-time spectroscopy in the mid-IR region. In addition to its use in spectroscopic measurements conducted in backscattering and transmission geometry, the MOEMS-based laser source is characterized regarding pulse intensity noise, wavelength reproducibility, and spectral resolution. [DOI: 10.1117/1.OE.57.1.011010]

Keywords: quantum cascade laser; microoptoelectromechanical systems; external cavity laser; mid-IR spectroscopy; real-time spectroscopy.

Paper 170919SSP received Jun. 14, 2017; accepted for publication Aug. 16, 2017; published online Sep. 12, 2017.

1 Introduction

The mid-IR spectral region from 3 to 12 μm is of particular interest for spectroscopic applications as molecules have their ro-vibrational transitions within this energy range. These transitions appear as a characteristic spectral absorption pattern, ideally suited for identification of molecules or functional groups. The availability of wavelength-tunable mid-IR lasers has opened up a variety of new applications of mid-IR spectroscopy.[1–6] Compared to incoherent light sources such as glow bars or LEDs, tunable lasers have various key advantages, e.g., exceptional spectral power density and resolution, and an almost diffraction limited, collimated output beam. Compact and rugged devices based on semiconductor lasers bear great potential as an enabling technology to transfer mid-IR spectroscopy from laboratory analysis to field use. In the mid-IR, quantum cascade lasers are ideally suited for this task,[7] complemented by interband cascade lasers at short wavelengths (3 to 5 μm).[8,9] The spectral coverage obtainable with a single quantum cascade laser (QCL) chip has significantly improved over the past few years.[10–12] Ever-increasing coverage increases molecular specificity by enabling the acquisition of more of the characteristic spectral fingerprint and increases instrument utility by making it sensitive to a larger range of molecules. External cavity configurations with wavelength-selective feedback are the most common approaches to exploit the full tuning range provided by the QCL chip. Also, distributed-feedback laser arrays have been used to realize broadly tunable QCL sources.[13]

*Address all correspondence to: Lorenz Butschek, E-mail: Lorenz. Butschek@iaf.fraunhofer.de

In addition to large tuning ranges, many applications require high scanning speeds of the laser wavelength, especially in nonstatic scenarios. Chemical reactions or moving objects can only be monitored by spectroscopic systems with sufficiently high spectral scanning speeds. Another interesting application of fast tunable lasers is handheld sensing devices that have to account for inevitable slight movements of the hand holding the device, and consequently the beam directed at the sample.

There have been several advances regarding the spectral scanning speed of EC-QCLs, e.g., a folded Littrow-type external cavity with a piezo-driven intracavity mirror by Tsai and Wysocki,[14] achieving tuning ranges of up to 7 cm^{-1} with a scan rate of 5 kHz. In a similar setup, Hugger et al.[15] employed a MOEMS mirror driven resonantly at 6 kHz (167 μs per cycle), scanning from 1070 to 1240 cm^{-1} within 84 μs. Lyakh et al. incorporated an acousto-optic modulator in the external cavity[16,17] and obtained a spectrum spanning 110 cm^{-1} in 17 μs.[18]

In this paper, we report on recent results obtained with our fast scanning EC-QCL system,[19–21] employing a MOEMS grating optimized specifically for broad spectral tuning in the mid-IR. The MOEMS grating is resonantly driven at a rate of 1 kHz. This approach significantly reduces weight and volume of the overall laser source to the point at which its ruggedness and the very low-power consumption of the MOEMS scanner also allow for the realization of handheld applications for in-field deployment.

Sections 2 and 3 provide a description and characterization of the laser source. In Sec. 4, various spectroscopic measurement scenarios employing the MOEMS EC-QCL are presented to demonstrate its real-time capabilities.

2 Microoptoelectromechanical Systems-Based Miniaturized External Cavity Laser

The MOEMS EC-QCL is based on different QCL chips designed and grown at Fraunhofer IAF. For broadband tuning in the 7- to 10-μm range, chips based on a heterocascading active region design[21,22] are operated in pulsed mode. Continuous wave (cw) measurements are conducted using an active region design optimized for maximum gain rather than broad tuning range. An antireflective (AR) coating is applied on the laser facet facing the resonator to suppress lasing on internal chip modes. On both the front and back facets of the laser chip, collimation lenses with high numerical aperture are aligned under operating conditions and glued to the heatsink. The Littrow configuration [see Fig. 1(a)] is completed by the silicon-based MOEMS scanner grating acting as wavelength-selective element in the external cavity [Fig. 1(b)]. The electrostatically driven circular scanner plate (5-mm diameter) is suspended by torsional springs and capable of deflection amplitudes up to 10 deg, with an integrated piezoresistive position sensor unit.[23] A trapezoidal (V-groove shaped) diffraction grating was etched into the top of the scanner plate. The diffraction grating for the 7 to 10 μm range used in this contribution has a groove density of 133 lines/mm.

The electrostatic scanner is driven by a custom-made control electronics board, which provides a trigger signal synchronized to the scanner oscillation and retrieves the amplitude information from the integrated position sensor. That in turn is used to determine the angle of the MOEMS grating and thus the emission wavelength of the laser source at any given time, as well as to synchronize grating motion and data acquisition. More details on the design and fabrication of the MOEMS module can be found in Ref. 19.

Our first demonstrator module contains this package in a stable housing, including a miniaturized laser pulse driver, Peltier element for temperature stabilization, and control electronics for the MOEMS scanner [Fig. 1(c)]. The laser is operated at room temperature; therefore, no capsulation is needed.

Assuming harmonic, distortion-free oscillation of the grating, the emission wavelength of the laser source as a function of time is given by

$$\lambda(t) = 2g\,\sin\{\alpha_{\text{center}} + A\,\sin[2\pi f(t - t_0)]\}, \tag{1}$$

where g is the grating constant, α_{center} is the Littrow angle at zero crossing, A is the deflection amplitude of the MOEMS scanner, f is the oscillation frequency, and t_0 is the time of the zero-crossing of the grating. This formula is used to convert the recorded data stream to spectroscopic data. As a consequence of this nonlinear time-wavelength correlation, equidistant sampling in the time domain—as has been done in this work—does not lead to equidistant spectral sampling but rather to higher sampling densities at the edges of the tuning range. However, constant spectral sampling could in principle be accomplished by an adapted trigger scheme.

3 Characterization of the Microoptoelectromechanical Systems-External Cavity Quantum Cascade Lasers

3.1 *Setup*

Depending on the operation mode of the laser, different laser drivers are used. For pulsed operation, a short-pulse voltage driver capable of delivering pulses with a pulse length between 50 ns and 10 μs and a current of up to 3 Amperes is used. A dedicated QCL low-noise current driver (Wavelength Electronics QCL2000) drives the laser chip in the case of cw operation. To measure laser intensity, photovoltaic mercury cadmium telluride (MCT) detectors (VIGO System) are used, thermoelectrically cooled to about 210 K, with a rise time of <3 ns. A gated integrator (Stanford Research SR250) with variable gate delay and a gate width of 100 ns is employed for time-resolved measurements, and spectra are taken by an FTIR spectrometer (Bruker Vertex

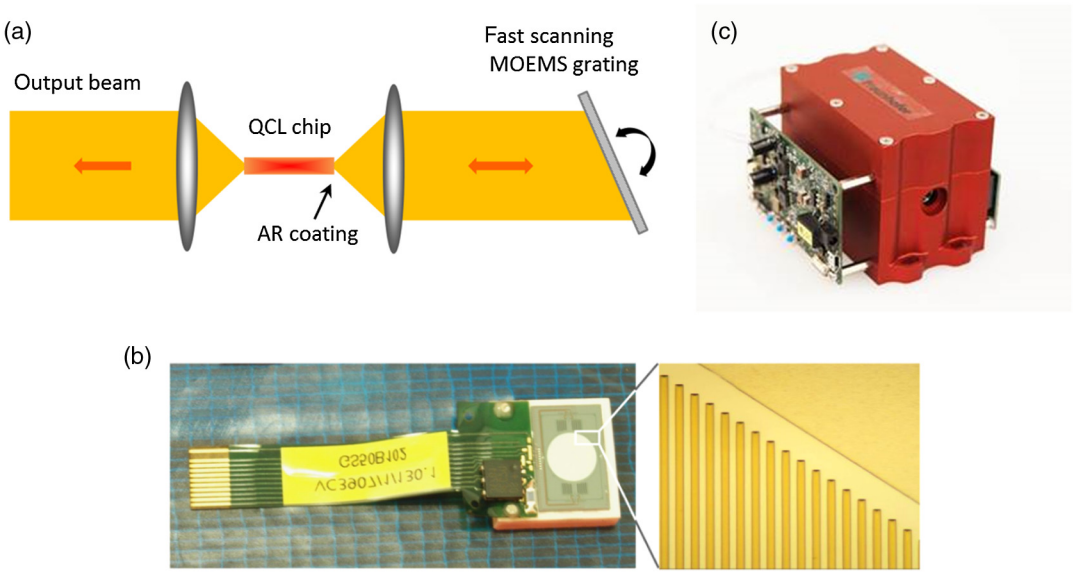

Fig. 1 Illustration of the laser source and its components:[20,21] (a) MOEMS EC-QCL in Littrow configuration. The distance from AR coated facet to MOEMS grating is <9 mm. (b) MOEMS scanner with etched grating. (c) Housing of the MOEMS EC-QCL module, including laser pulse driver, MOEMS control electronics, and temperature stabilization.

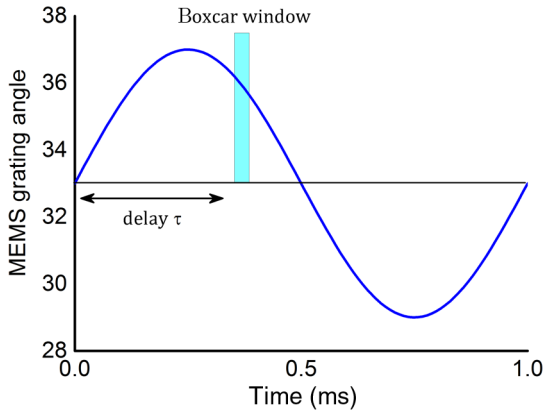

Fig. 2 The time dependence of the angle of a typical MOEMS grating is shown in blue. The rectangle indicates the boxcar window gating the detector at variable time delays from the MOEMS trigger. When operating the laser in pulsed mode, the laser pulse is timed accordingly.

80) with a fast MCT detector that allows for boxcar-integrated, time-resolved spectral characterization of the laser source.

Fast spectroscopy measurements as shown in Sec. 4 are conducted with the laser in pulsed mode driven with repetition rates of 400 to 500 kHz, yielding 400 to 500 spectral sampling points within the oscillation period of 1 ms. To reconcile the very rapid tuning rate of the laser to the slow measurement acquisition of the FTIR spectrometer when measuring the absolute optical frequency produced by the laser source as a function of MOEMS grating position, the acquisition of the FTIR detector was gated with variable delay with respect to the trigger signal produced by the MOEMS positional output (Fig. 2). This allows for slower data acquisition methods and time-resolved spectral investigations using an FTIR.

Figure 3(a) shows the tuning ranges of several chips in external cavity operation used for measurements shown in this paper, all with maximum peak power levels of several hundred mW. Figure 3(b) shows a transmission spectrum of a GaAs wafer with a thickness of 124 μm recorded with the MOEMS EC-QCL equipped with chip #2, exhibiting clearly visible interference fringes of the GaAs etalon.

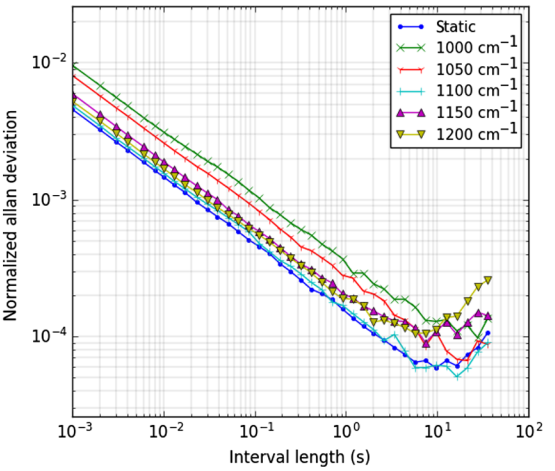

Fig. 4 Allan plots: two-sample deviation (Allan) plots of pulse intensity are shown to differentiate between short-term pulse intensity noise and long-term drift—measured with both static MOEMS scanner (emitting at 1105 cm^{-1}) and moving scanner. Starting at intervals of about 10 s, drift effects start to appear, corresponding to several thousand averaged spectra.

These fringes provide a quick and easy way to monitor the spectral tuning behavior, e.g., on an oscilloscope.

3.2 *Pulse-to-Pulse Fluctuations*

For an evaluation of the laser source with regard to pulse-to-pulse intensity fluctuations, chip #2 is driven with 100 ns pulses at fixed delays to the MOEMS trigger (i.e., fixed wavelengths). The integrated pulse intensity is then recorded for time periods of 5 min. Allan deviation plots[24,25] of the data are shown in Fig. 4. As long as short-term noise dominates over long-term drift, the inverse dependence of Allan deviation on averaging interval length appears as a straight line on the log–log scale. It is apparent that up to averaging intervals of about 10 s, no drift effects affect laser noise performance. Note that for a laser source aiming at real-time applications, the envisioned averaging interval times are much shorter (typically below 100 ms). For such interval lengths, the normalized standard deviation of mean pulse intensity is on the order of 10^{-3}. Allan deviation is measured

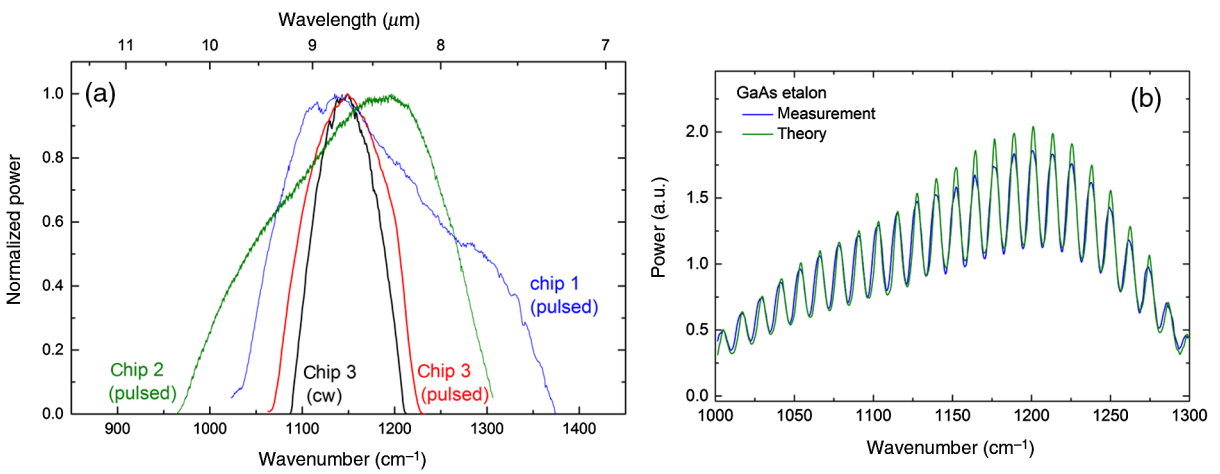

Fig. 3 (a) Power versus wavelength profiles of the chips used for the measurements reported here. (b) Transmission spectrum of a 124-μm thick GaAs etalon recorded with the rapid-scan MOEMS EC-QCL equipped with QCL chip #2.

in both static mode (i.e., with the scanner turned off) and dynamic mode. Using a variable gate delay of the boxcar integrator, multiple dynamic Allan plots are recorded at different wavelengths. Differences in overall noise level are tentatively attributed to the varying prevalence of mode hops at different grating angles.

3.3 *Linewidth and Spectral Reproducibility*

Spectral emission linewidth and wavelength reproducibility are among the most important characteristics of any laser source to be employed in spectroscopic applications. In pulsed operation, the typical spectral width[20] of its emission lies between 1 and 2 cm^{-1}. Changing to a cw-capable laser [chip #3, see Fig. 3(a)] allowed us to significantly reduce the spectral width of its emission. The laser is driven with 800 mA of cw current and stabilized at a heatsink temperature of 20°C. Spectra are taken using the gated spectrometer and boxcar integrator, measured at different times of the scanner oscillation by tuning the time delay between MOEMS trigger signal and boxcar window (100 ns gate width). An exemplary spectrum of the cw MOEMS EC-QCL is displayed in Fig. 5 (blue), exhibiting a spectral width of FWHM = 0.27 cm^{-1}, limited by the resolution of our FTIR spectrometer. The spectrum taken with a static scanner (i.e., actuation of the scanner turned off, grating in its rest position) exhibits the same, instrument-limited linewidth. Obviously, the scanner movement does not impair the linewidth over the measurement time of about 30 s it takes to record one FTIR spectrum. From these measurements, it can be inferred that the spectral reproducibility of the MOEMS EC-QCL within that time frame is better than the spectral resolution of the FTIR (0.27 cm^{-1}).

The time-dependent wavelength of the cw emission is investigated by varying the time delay between MOEMS trigger signal and boxcar window in small steps and plotting the center of the respective emission peaks as function of the delay, as shown in Fig. 6. Marked by black dots are the center wavelengths of the respective main emission peaks at a certain timestamp. The blue line represents the sinusoidal curve according to the grating equation (see Sec. 2) and the respective scan parameters. Note that amplitude and phase of the scanner oscillation were obtained by fitting Eq. (1) to the data. No indications for a deviation from the assumed sinusoidal motion of the scanner are found. A more detailed view reveals individual longitudinal mode-hops in steps of about 0.75 cm^{-1} during the spectral scan. This effect results from the coupled cavity that consists of the external resonator and the laser chip acting as a weak Fabry–Perot resonator (chip length of 2 mm, refractive index $n = 3.33$).

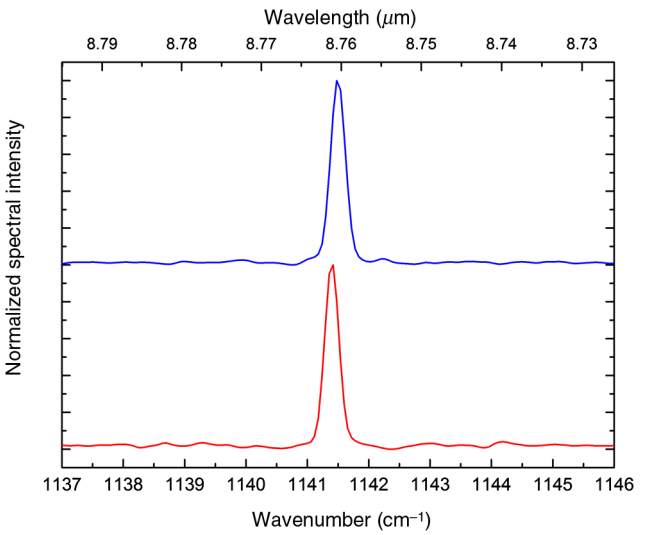

Fig. 5 Lasing spectra in cw operation: Shown in blue is an example of an emission spectrum of the MOEMS EC-QCL in cw operation at a specific timestamp. For comparison, the spectrum of the static laser source is plotted in red. The linewidths (FWHM = 0.27 cm^{-1}) are the same, limited by the resolution of the FTIR spectrometer.

4 Real-Time Spectroscopy

To demonstrate the capabilities and versatility of the MOEMS EC-QCL as a spectroscopic light source, we performed different types of spectroscopic measurements described in the following section.

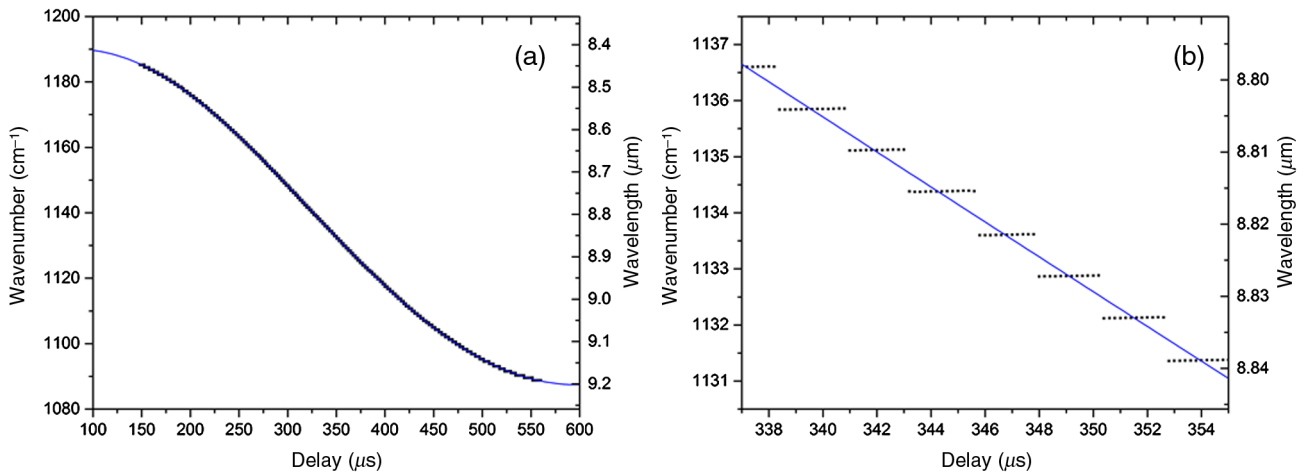

Fig. 6 Mapping of the time-dependent emission wavelength: (a) center wavelengths of the main emission peaks are plotted against the respective delays between MOEMS trigger and boxcar window (black dots). The zero-crossing of the grating occurs at an arbitrary 321 μs after the trigger signal. The blue line shows the expected emission wavelength derived from Eq. (1). (b) Zooming into the plot resolves the longitudinal mode hops in steps of about 0.75 cm^{-1}.

4.1 *Backscattering Spectroscopy*

The first application to be discussed is contactless ("stand-off") identification of chemical substances on surfaces over a certain distance by diffuse reflectance spectroscopy.

In previous publications, we investigated this topic in a security-related context with the means of hyperspectral imaging using a slow-scanning EC-QCL for active illumination of the scene and a high-end MCT camera for collecting the backscattered radiation. With a tripod-mounted system with a large-aperture collection optics, small amounts of explosives and related precursors could be detected over distances of about 20 m with spectral scanning times on the order of 10 to 30 s.[20] Here, we present our first results obtained with a QCL-based handheld scanner designed to detect a wide range of substances on arbitrary surfaces over shorter distances of about 0.5 to 2 m. These developments are driven by the need of first responders for portable and simple-to-use detection hardware for fast identification of suspicious, potentially hazardous substances. Importantly, the technique works at eye-safe power levels. The MOEMS EC-QCL represents an ideal laser source for a handheld device, as one main challenge (in addition to the obvious requirement of a compactness and low weight) are slight, unavoidable movements of the hand holding the device and hence the laser beam. This issue can be solved by fast spectral scanning, as every single spectrum is collected in a time short enough to consider the beam stationary. Recently, we performed measurements in a comparable laboratory optical setup situation, where laser and detector were still fixed on an optical table, and the sample was moved manually during measurement to mimic the handheld-situation.[19] Here, we present, for the first time, results using a handheld device.

The handheld demonstrator (Fig. 7) contains a MOEMS EC-QCL as light source, equipped with a QCL chip tunable from 1000 to 1300 cm^{-1}. The laser is operated in pulsed mode at ~500 kHz, 100 ns. The sample is illuminated with a collimated beam of ~5-mm diameter. The beam is collinear with the optical axis of the receiver optics, a 4 in. $f/2$ mirror that collects and focuses the diffusely scattered light onto a fast, thermoelectrically cooled MCT detector (Vigo System). In this first demonstrator, the operating distance was fixed to 1 m, with the signal remaining above 85% within a total defocus range of ~10 cm. Beam position and working distance are indicated to the operator by two visible laser diodes crossing their beams in the focal plane of the receiver optics. A forward facing camera and rear-facing monitor are provided for operator feedback. The most recent constantly acquired spectrum is displayed in real time, along with the forward facing field of view.

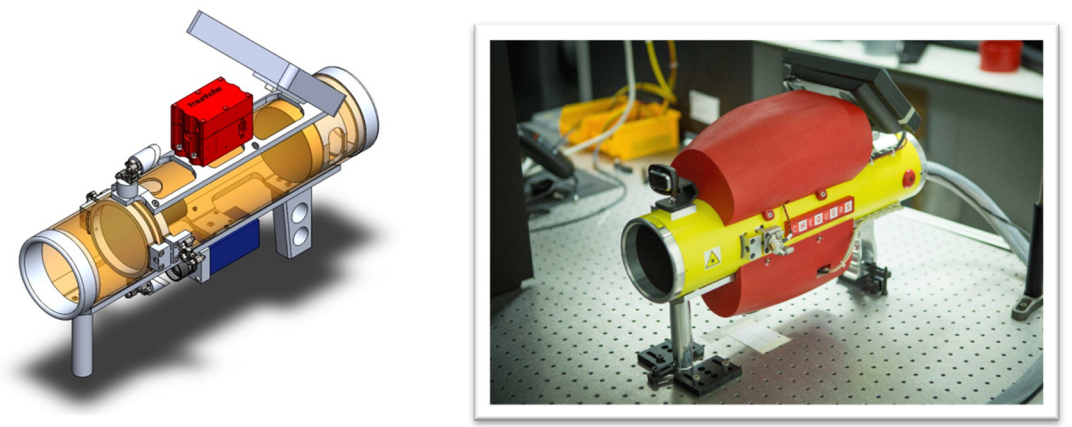

Fig. 7 Portable demonstrator for contactless detection of solids. The MOEMS EC-QCL is located on top of the device, the single-element MCT detector at the bottom.

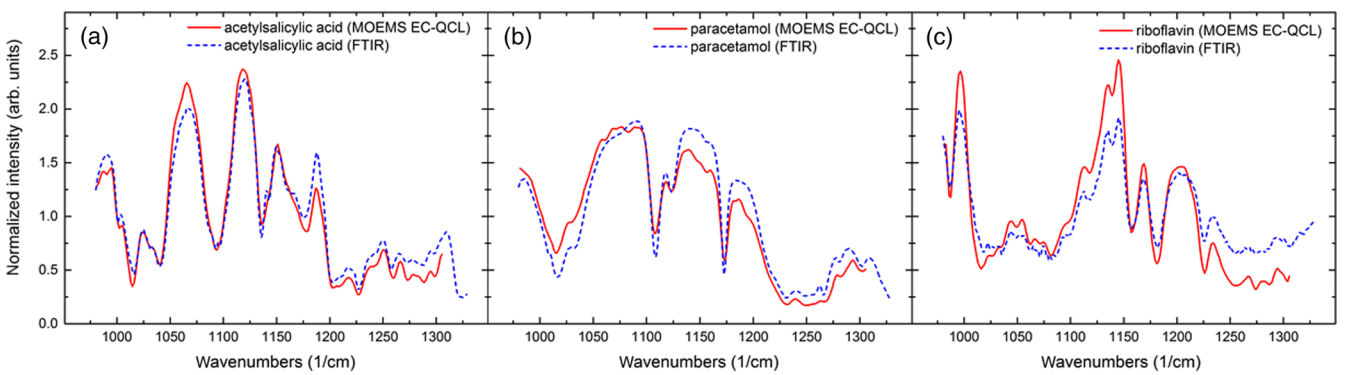

Fig. 8 Diffuse reflectance spectra of bulk samples from (a) acetylsalicylic acid, (b) paracetamol and (c) riboflavin obtained with a MOEMS-ECL-based scanner (500 ms acquisition time, i.e., 500 averaged spectra, 1 m distance), and with an FTIR microscope (acquisition time of several minutes), respectively. The results are well comparable.

In Fig. 8, we show that diffuse reflectance spectra measured with this device are well comparable to those obtained by established reflectance spectroscopy using an IR microscope coupled to an FTIR.

Samples as shown in Fig. 8 could be identified with our handheld scanner in quasi real-time by comparing the recorded spectra with a database, using a simple and very fast cross-correlation algorithm (not shown). While this approach is successful on bulk samples (i.e., strong coverage of the underlying substrate), detection of residual material on scattering substrates often poses the problem of background interference, i.e., significant contributions of the *a priori* unknown substrate to the recorded spectrum. In previous work on imaging detection, we showed that this can be accounted for by suitable data analysis, if a hyperspectral image (spatially resolved spectral information over a certain area) of the sample is available and contains uncontaminated pixels providing the respective background spectrum.[26] Here, such a dataset is obtained by scanning the beam manually over a sample of polyamide contaminated with the explosive pentaerythritol tetranitrate (PETN) for a few seconds. The sample and approximated path of the beam are shown in Fig. 9(a). Figure 9(b) shows color-coded time-resolved spectra taken during the recording process. Each column is treated as a pixel of a hyperspectral image by our target detection algorithms, described in detail e.g., in Ref. 26. Here, we want to point out that the only necessary input is the target spectrum while the unknown background is extracted from the dataset by the algorithm. The top row of Fig. 9(b) shows the time-resolved detection results. In Fig. 9(d), the spectra obtained in regions considered as "PETN contaminated" as well as in uncontaminated regions are shown. Despite strong contributions of the polyamide background present in all spectra, PETN is identified, and the spectrum of pure PETN is recovered from the data by spectral unmixing [Fig. 9(c)]. Similar results were obtained with other hazardous contaminations and substrates.

We note that the described approach does not deliver actual "real-time" results as in the case of cross correlation, analyzing single spectra. First, the spatial scan has to be completed, as our background-suppressing algorithm requires the entire dataset.

Current work on the optical part includes implementation of an autofocus for variable distance measurement and reducing the overall size. Furthermore, data acquisition and analysis, which took place on a separate computer, will be integrated in the device to provide a truly mobile scanner.

4.2 *Transmission Spectroscopy for Quality Control of Coatings*

In our second example, we demonstrate how the MOEMS-EC QCL can be used to monitor coating quality. A potential,

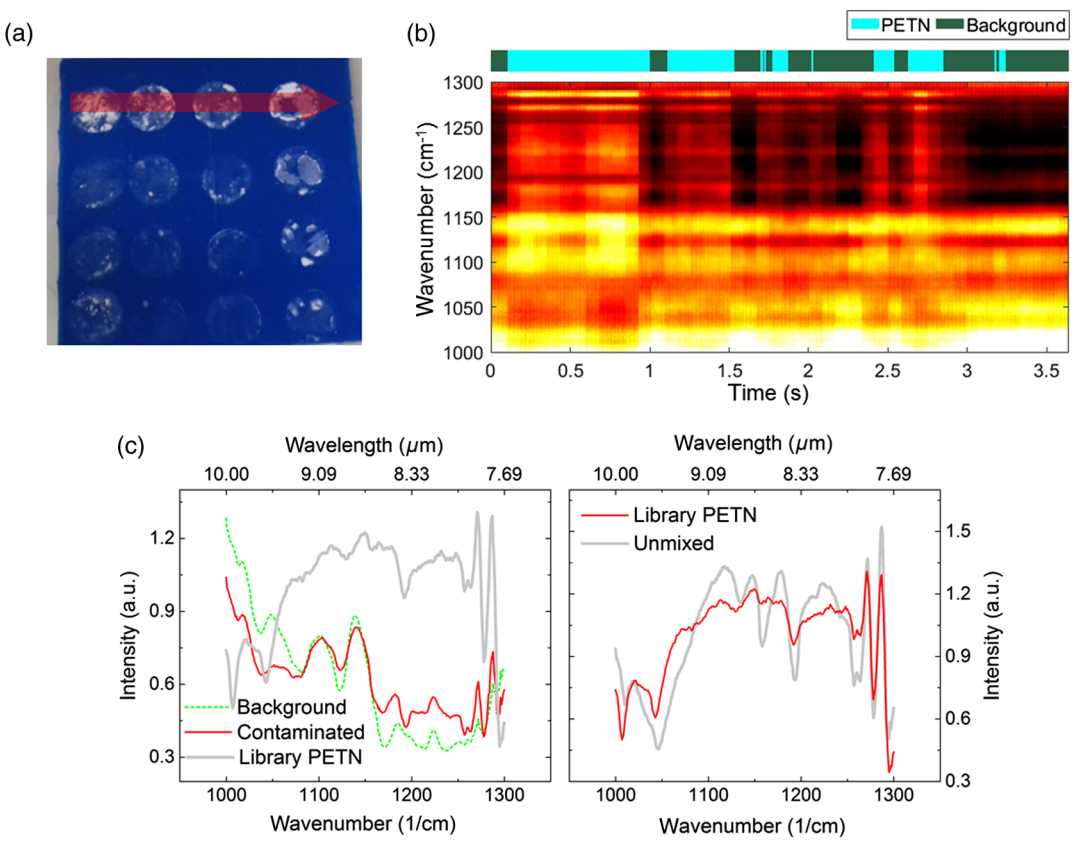

Fig. 9 (a) Sample: PETN contaminations on polyamide substrate. The arrow shows the approximated trace of the laser beam on the sample during manual scanning. (b) Color-coded evolution of the spectra obtained while the beam is scanned over the sample for ~3.5 s. In the top row, detection results obtained with the adaptive matched subspace detection algorithm[26] applied to the whole dataset are displayed. (c) Left: averaged spectra of regions classified as PETN contaminated (red), uncontaminated (green), and our PETN library spectrum used for detection. Right: the PETN library spectrum is recovered from the data after unmixing using our detection algorithms.

challenging, and timely example of in-line monitoring using our technology is the application of a coating such as glue or silicone to a thin foil, or the detection of contaminations (oil, silicone, etc.) on a foil before the coating process. Such applications with industrial context typically require high measurement speeds to achieve sufficient spatial resolution on fast moving samples.

We prepared a silicone coating with intentional defects (i.e., gaps) on a polyethylene foil by manual spray coating. The foil is glued to a chopper wheel, which allows moving the sample at predefined velocities. The foil is measured in transmission geometry with the laser beam being focused on the foil (NA ~ 0.05) to ensure high spatial resolution. The chopper wheel has five segments containing [see Fig. 10(a)] A. PE foil, B. silicone on PE with a 6-mm-wide line defect, C. silicone on PE with 4-mm defect, D. silicone on PE with 3-mm defect, and E. silicone on PE with 2-mm defect. In Fig. 10(b), we show the measured transmission spectra versus time for a scan velocity of 0.5 m/s. Spectra recorded while the laser was blocked by the spokes of the chopper wheel were removed, as they contain no useful information (zero transmitted intensity). All spectra are referenced to a PE foil with no coating applied. The spectra from segment A are an indicator for the deviations of the PE foil thickness from the reference foil.

In Fig. 10(c), we compare a single transmission spectrum of the silicone coating measured with the MOEMS EC-QCL with an FTIR reference measurement for the same sample. The silicone coating exhibits several strong absorption bands in the considered spectral range of 1000 to 1300 cm^{-1}. Using the strongest absorption bands, a simple quality parameter was constructed. In Fig. 10(d), we plot the quality parameter. All defect lines, including those with the smallest width of 2 mm could be identified. It becomes obvious that the coating thickness varies strongly throughout the sample due to our manual coating process. However, from the measured spectra, a limiting value distinguishing between a good and faulty or not existing coating can be defined.

We note that in Fig. 10(d), each point corresponds to a single spectral scan. The spatial resolution for a velocity of 0.5 m/s is ~0.5 mm along the moving direction using the full MOEMS scan period of 1 ms for the construction of one spectrum, as has been done here. During one such period the full spectral range is covered twice (once in either direction), therefore the above spatial resolution could be doubled. For the smallest defect of 2-mm width, this causes a deviation of the quality parameter in four consecutive IR spectra, which matches well with the experimental results. The evaluation of the full spectral dataset allows for an increased signal-to-noise ratio and less dependence on other changing parameters such as changes in the foil thickness due to the fast and fluttering movement of the sample.

4.3 *Transmission Spectroscopy of Gases*

Our third example is real-time absorption spectroscopy in the gaseous phase.[19] In its present form, the MOEMS EC-QCL

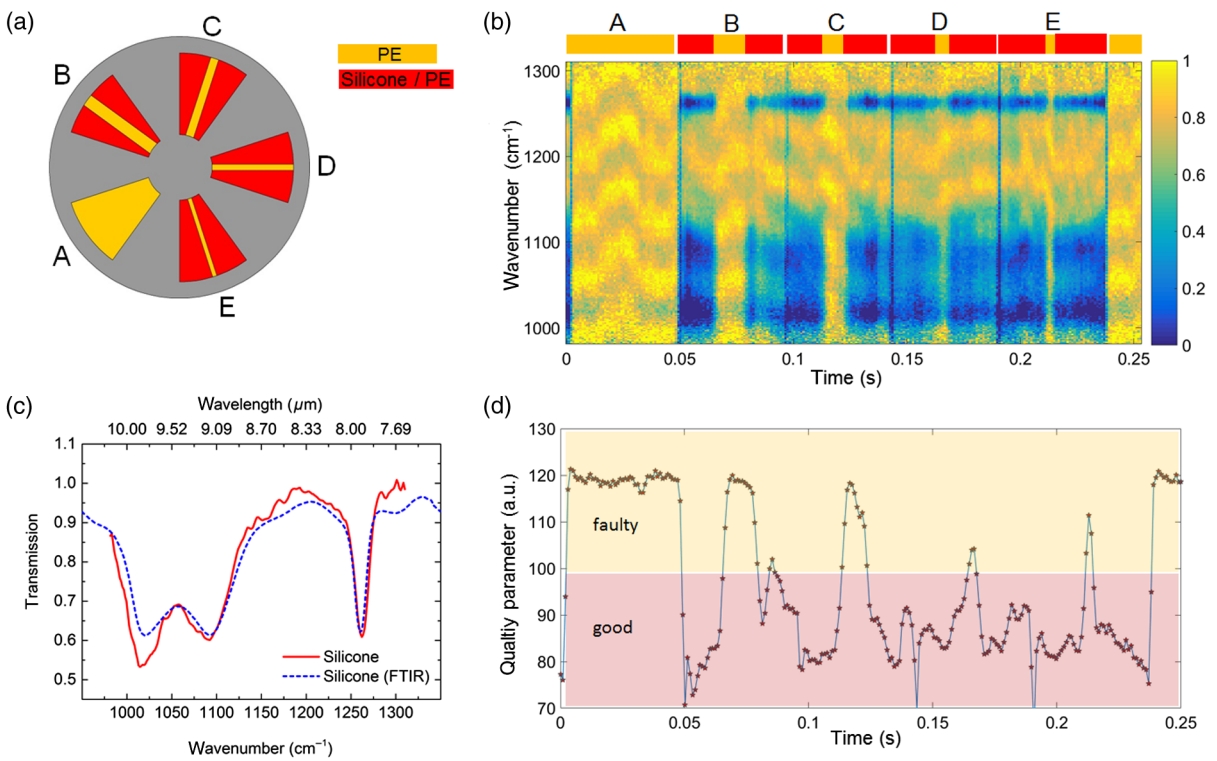

Fig. 10 (a) Sample: each of the five compartments of a chopper wheel contains a PE foil, patterned with a silicone coating with intentional line defects of width 6, 4, 3, and 2 mm, as indicated above. The sample was measured while moving at 0.5 m/s at the beam position. (b) Color-coded evolution of the relative transmission spectra. The transmission is referenced to an uncoated PE foil. Spectra recorded while the laser was blocked by the spokes of the chopper wheel were removed. (c) Single spectral scan of the silicone coating using the MOEMS EC-QCL versus an FTIR reference measurement of the same sample. (d) Quality parameter constructed from the spectra in (b). A threshold can be chosen to define a faulty coating.

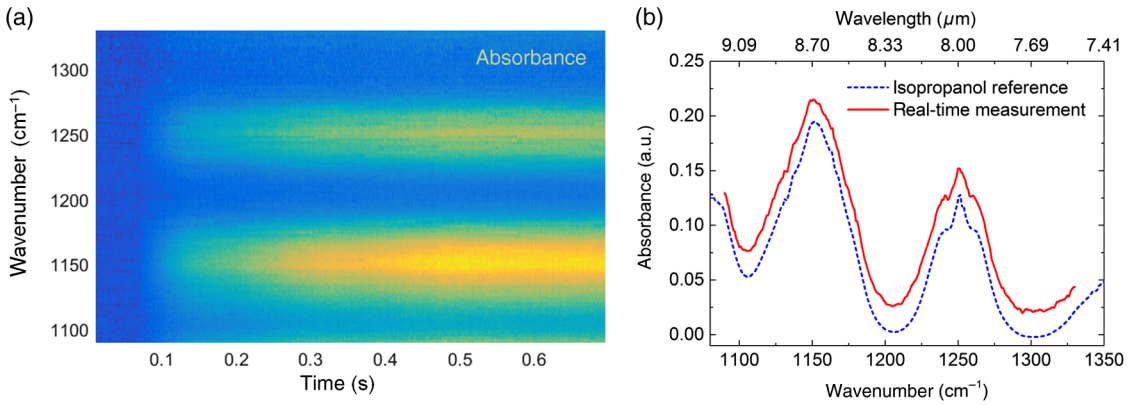

Fig. 11 (a) Time-resolved color-coded representation of the measured absorbance spectrum, recorded while air saturated with isopropanol vapor is blown into an integration sphere (see text). Data have been referenced to the initial state (no isopropanol present). Changes in absorbance appear on short timescales of ~10 ms, saturation is approached after ~0.5 s. (b) Measured absorbance spectrum after 0.5 s (in red), showing a very good match to literature data in blue (from NIST,[27] scaled to our data to account for different path length and offset by 0.02 for better visual comparison).

is not intended for high-resolution spectroscopy of narrow gas absorption lines. While narrow linewidth can be provided in cw operation, length adjustment of the resonator during a wavelength scan is currently not implemented; therefore, the laser will undergo mode-hops during spectral scanning, as shown in Sec. 3.3. However, the absorption spectra of some gases consist of somewhat broader absorption bands, and these gases are well suited to be probed by a pulsed laser source with a spectral resolution on the order of 1 cm^{-1}. The MOEMS EC-QCL allows fast tracking of changes in gas concentration as shown below. Note that also in a scenario where the main concern is not real-time monitoring but mere detection of some gaseous compounds, fast spectroscopy can still be very valuable. In turbulent media, for instance, spectra taken over longer periods than occurring changes in composition are very difficult, if not impossible, to interpret. These issues are avoided by fast spectral scanning, as every single recorded spectrum is meaningful.

Here, we chose isopropanol vapor as a model gas with two broad spectral features in the 7.5- to- 9 μm range. The beam of the MOEMS EC-QCL equipped with chip #1 is directed at an integrating sphere. Its intensity is recorded with a fast MCT detector placed at the exit port of the sphere. Air saturated with isopropanol vapor is blown through a small hole into the integrating sphere that also acts as a very simple means to increase the absorption length as the laser light undergoes multiple internal reflections before reaching the detector. The temporal evolution of the recorded absorbance spectra is shown in Fig. 11(a). In Fig. 11(b), the measured absorbance after saturation is depicted, showing very good agreement to literature data for isopropanol vapor (from Ref. 27).

5 Summary

We presented recent results obtained with an EC-QCL module equipped with custom-made MOEMS scanning gratings in Littrow configuration. The MOEMS scanning grating is operated at its resonance frequency of 1 kHz and covers the whole spectral range of our QCL chips (>300 cm^{-1}) in 500 μs. The MOEMS EC-QCL was characterized in pulsed and cw mode with regard to spectral reproducibility and pulse-to-pulse fluctuations. Spectral fluctuations in dynamic operation were found to be below 0.27 cm^{-1} over 30 s, measured in cw mode. Pulse-to-pulse fluctuation showed no drift effects on timescales of several seconds, significantly more than necessary for real-time measurements. Furthermore, we employed the MOEMS EC-QCL as a spectroscopic light source to perform real-time spectroscopy in different prototypical application scenarios: stand-off backscattering spectroscopy using a handheld scanner was presented, including identification of a target compound on an interfering substrate. In future work, we will refine the optical design and utilize coated plastic optics to reduce the size and mass of the instrument, and implement an autofocus mechanism to allow for more flexible use in end-use environments. Transmission spectroscopy in nonstatic scenarios was demonstrated in two examples: defects as small as 2 mm in width in a silicone coating on a PE foil could be detected while the sample was moving at 0.5 m/s. Rapidly occurring changes in isopropanol gas concentrations could be reliably tracked while isopropanol vapor was blown into an integration sphere.

Acknowledgments

Part of the research leading to these results has received funding from the European Community's Seventh Framework Program (FP7/2007-2013) under Grant Agreement Nos. 317884 MIRIFISENS and the Horizon 2020 Program under Grant Agreement Nos. 645535 CHEQUERS and 688265 MIRPHAB. The authors want to thank Q. Yang, R. Aidam, W. Bronner, R. Driad, and U. Weinberg for expert design, fabrication, and testing of the QCL chips used in the presented experiments, and C. Schilling for expert technical assistance. We acknowledge supply of the MCT detector for the handheld scanner by M. Ratajczyk (Vigo System) and helpful discussion with R. Schulte-Ladbeck, T. Fröhlich (Bundeskriminalamt BKA), and J. Bain (M squared lasers) under the support of the H2020 CHEQUERS project.

References

1. G. Wysocki et al., "Widely tunable mode-hop free external cavity quantum cascade lasers for high resolution spectroscopy and chemical sensing," *Appl. Phys. B* **92**(3), 305–311 (2008).

2. M. Kölhed et al., "Assessment of quantum cascade lasers as mid infrared light sources for measurement of aqueous samples," *Vib. Spectrosc.* **29**(1), 283–289 (2002).
3. K. Wörle et al., "Breath analysis with broadly tunable quantum cascade lasers," *Anal. Chem.* **85**(5), 2697–2702 (2013).
4. A. Lambrecht et al., "Broadband spectroscopy with external cavity quantum cascade lasers beyond conventional absorption measurements," *Analyst* **139**(9), 2070–2078 (2014).
5. T. F. Beskers et al., "High performance liquid chromatography with mid-infrared detection based on a broadly tunable quantum cascade laser," *Analyst* **139**(9), 2057–2064 (2014).
6. M. C. Phillips et al., "Real-time trace gas sensing of fluorocarbons using a swept-wavelength external cavity quantum cascade laser," *Analyst* **139**(9), 2047–2056 (2014).
7. A. Hugi, R. Maulini, and J. Faist, "External cavity quantum cascade laser," *Semicond. Sci. Technol.* **25**(8), 083001 (2010).
8. I. Vurgaftman et al., "Interband cascade lasers with low threshold powers and high output powers," *IEEE J. Sel. Top. Quantum Electron.* **19**(4), 1200210 (2013).
9. R. Weih et al., "Single mode interband cascade lasers based on lateral metal gratings," *Appl. Phys. Lett.* **105**(7), 071111 (2014).
10. A. Hugi et al., "External cavity quantum cascade laser tunable from 7.6 to 11.4 μm," *Appl. Phys. Lett.* **95**, 061103 (2014).
11. P. Rauter and F. Capasso "Multi-wavelength quantum cascade laser arrays," *Laser Photonics Rev.* **9**(5), 452–477 (2015).
12. W. Zhou et al., "Monolithically, widely tunable quantum cascade lasers based on a heterogeneous active region design," *Sci. Rep.* **6**, 25213 (2016).
13. N. Bandyopadhyay et al., "Ultra-broadband quantum cascade laser, tunable over 760 cm^{-1}, with balanced gain," *Opt. Express* **23**(16), 21159–21164 (2015).
14. T. Tsai and G. Wysocki "External-cavity quantum cascade lasers with fast wavelength scanning," *Appl. Phys. B* **100**(2), 243–251 (2010).
15. S. Hugger et al., "Broadband-tunable external-cavity quantum cascade lasers for the spectroscopic detection of hazardous substances," *Proc. SPIE* **8631**, 86312I (2013).
16. A. Lyakh et al., "Continuous wave operation of quantum cascade lasers with frequency-shifted feedback," *AIP Adv.* **6**(1), 015312 (2016).
17. A. Lyakh et al., "Progress in rapidly-tunable external cavity quantum cascade lasers with a frequency-shifted feedback," *Photonics* **3**(2), 19 (2016).
18. A. Lyakh et al., "External cavity quantum cascade lasers with ultra rapid acousto-optic tuning," *Appl. Phys. Lett.* **106**(14), 141101 (2015).
19. J. Grahmann et al., "Tunable external cavity quantum cascade lasers (EC-QCL): an application field for MOEMS based scanning gratings," *Proc. SPIE* **8977**, 897708 (2014).
20. R. Ostendorf et al., "Recent advances and applications of external cavity-QCLs towards hyperspectral imaging for standoff detection and real-time spectroscopic sensing of chemicals," *Photonics* **3**(2), 28 (2016).
21. L. Butschek et al., "Real-time spectroscopy enabled by external cavity QCLs with MOEMS diffraction gratings," *Proc. SPIE* **10111**, 101112G (2017).
22. R. Maulini et al., "External cavity quantum-cascade lasers tunable from 8.2 to 10.4 μm using a gain element with a heterogeneous cascade," *Appl. Phys. Lett.* **88**(20), 201113 (2006).
23. J. Grahmann et al., "MEMS-mirror based trajectory resolution and precision enabled by two different piezoresistive sensor technologies," *Proc. SPIE* **9760**, 976006 (2016).
24. P. O. Werle, R. Mücke, and F. Slemr, "The limits of signal averaging in atmospheric trace-gas monitoring by tunable diode-laser absorption spectroscopy (TDLAS)," *Appl. Phys. B* **57**(2), 131–139 (1993).
25. P. Werle, "Accuracy and precision of laser spectrometers for trace gas sensing in the presence of optical fringes and atmospheric turbulence," *Appl. Phys. B* **102**(2), 313–329 (2011).
26. J. Jarvis et al., "Hyperspectral data acquisition and analysis in imaging and real-time active MIR backscattering spectroscopy," *Adv. Opt. Technol.* **6**(2), 85–93 (2017).
27. P. M. Chu et al., "Quantitative infrared database," NIST Chemistry WebBook, NIST Standard Reference Database Number 69, P. J. Linstrom and W. G. Mallard, Eds., National Institute of Standards and Technology, http://webbook.nist.gov.

Lorenz Butschek received his diploma degree in physics from the University of Innsbruck, Austria, in 2014. He has been working as a PhD student at the Fraunhofer Institute for applied solid state physics (IAF) in Freiburg, Germany, on miniaturized external cavity QCLs. His current research focuses on spectral stability and intensity noise for spectroscopic applications.

Stefan Hugger received his diploma in physics from the University of Freiburg, Germany, in 2003 and his PhD in physics from the University of Düsseldorf, Germany, in 2008. He joined the Fraunhofer Institute for Applied Solid State Physics in Freiburg, Germany, in 2008. His current research focuses on external cavity QC lasers and their applications in spectroscopy.

Jan Jarvis received his diploma in computer science from Karlsruhe Institute of Technology in 2011. He has been working at Fraunhofer IAF on stand-off spectroscopy using active QCL-based hyperspectral imaging for detection of hazardous substances. His current research interest lies in data analysis, statistical modeling, and signal processing.

Marko Haertelt received his diploma degree in physics from TU Berlin in 2008. He worked as a research assistant at the Fritz Haber Institute of the Max Planck Society in Berlin, Germany, from 2008 to 2012 and received his PhD in physics in 2012. From 2012 to 2015, he worked as a postdoctoral fellow at the Joint Attosecond Science Laboratory of the University of Ottawa and National Research Council Canada. He joined Fraunhofer IAF in 2016.

André Merten received his diploma degree in physics from Friedrich-Schiller-University Jena in 2003. After that, he was a PhD student at the University of Heidelberg and worked on differential optical absorption spectroscopy (DOAS) of atmospheric trace gases and received his PhD in 2008. Afterward, he joined the Technical University in Dresden and worked on thin film organic solar cells. Since 2012, he has worked at the Fraunhofer IPMS on optomechanical system design involving MEMS scanners.

Markus Schwarzenberg received his PhD at the Technical University of Dresden. He was working in various fields of information technology, such as speech synthesis, signal processing, electronics, and software development; he is currently leading an MEMS application-oriented hard- and software development team at the Fraunhofer IPMS Dresden.

Jan Grahmann defended his dissertation, "Highly sensitive resonant gas sensors based on single crystal plate-oscillators," at the University of Chemnitz in 2008 and joined the Fraunhofer IPMS in 2007. He has been working in the field of micromechanical scanning mirrors and managed international public and industrial projects. He became head of the Micro Scanner Device Development Group in 2010 and has been managing the business unit AMS since 2013.

David Stothard has pioneered the development and application of compact, high efficiency, broadly tunable intracavity optical parametric oscillators. This, together with the realization of advanced scanning geometries, has enabled the ICOPO to be applied to a wide range of hyperspectral imaging scenarios and led to the development of numerous technological embodiments of the source and scanning technologies. His other interests include the development of single frequency, broadly mode-hop free tunable lasers, and electronic instrumentation.

Matthew Warden performs industrially focused research into laser-based sensing and measurement systems. This has included precision position measurement for production engineering, remote wind speed measurement for renewable energy, chemical sensing for security applications, and spectroscopy for medical applications. His focus is on modeling and optimization of system performance, and on improving measurement quality through improved analysis methods.

Christopher Carson presently works on mid-IR laser sources and sensing applications, as well as compact, efficient and novel lasers, and laser systems for atom/ion trapping, cooling, and applications. His range of research also includes the design and development of compact, rugged and reliable laser systems for cold atom/ion applications (such as space application, atom interferometers, and optical clocks).

John Macarthur recently has been developing instrumentation of devices for laser beam characterization measurements, m2, wavelength spectrum, and frequency composition as well as systems for stand-off imaging and spectroscopy applications. He has also been investigating novel feedback solutions to control the shape of Q-switched laser pulses to be used as seed sources.

Frank Fuchs joined the Fraunhofer IAF more than 30 years ago, working on infrared devices based on InAs/GaSb type II heterostructures

and quantum cascade lasers. Since 2007, he was leading several projects dealing with stand-off detection of explosives. His published work comprises about 120 papers. He presented his work in more than 20 invited talks on international conferences. Since 2017, he has been working as a research consultant.

Ralf Ostendorf received his PhD in physics from the University of Muenster, Germany, in 2005. In 2007, he joined the Fraunhofer IAF in Freiburg, Germany, where he developed GaAs-based diode lasers. In 2009, he started working in the development of external cavity quantum cascade lasers in the mid-IR with focus on application in sensing systems. Since 2016, he has been the head of the business unit "semiconductor lasers" at Fraunhofer IAF.

Joachim Wagner received his PhD in physics from Stuttgart University, Germany, in 1982. He joined the Fraunhofer Institute for applied solid state physics, Freiburg, Germany, in 1985, where he is currently acting executive director. He is also a professor at the Institute of Physics of the University of Freiburg. His current research interests include III/V-semiconductor-based optoelectronic devices and their integration into modules and sensing systems. He is the author or coauthor of 470 scientific publications.